

New Limits on Neutrino Magnetic Moments from the Kuo-Sheng Reactor Neutrino Experiment

H.B. Li,^{1,2} J. Li,^{1,3,4} H.T. Wong,^{1,*} C.Y. Chang,^{1,5} C.P. Chen,¹ J.M. Fang,⁶ C.H. Hu,⁷ W.S. Kuo,⁷ W.P. Lai,^{1,8}
F.S. Lee,¹ S.C. Lee,¹ S.T. Lin,¹ C.S. Luo,¹ Y. Liu,³ J.F. Qiu,^{1,3} H.Y. Sheng,^{1,3} V. Singh,¹ R.F. Su,⁶ P.K.
Teng,¹ W.S. Tong,⁷ S.C. Wang,¹ B. Xin,^{1,9} T.R. Yeh,⁷ Q. Yue,³ Z.Y. Zhou,⁹ and B.A. Zhuang^{1,3}

(TEXONO Collaboration)

¹ Institute of Physics, Academia Sinica, Taipei 115, Taiwan.

² Department of Physics, National Taiwan University, Taipei 106, Taiwan.

³ Institute of High Energy Physics, Beijing 100039, China.

⁴ Department of Engineering Physics, Tsing Hua University, Beijing 100084, China.

⁵ Department of Physics, University of Maryland, College Park MD 20742, U.S.A.

⁶ Kuo-Sheng Nuclear Power Station, Taiwan Power Company, Kuo-Sheng 207, Taiwan.

⁷ Institute of Nuclear Energy Research, Lung-Tan 325, Taiwan.

⁸ Department of Management Information Systems, Chung Kuo Institute of Technology, Hsin-Chu 303, Taiwan.

⁹ Department of Nuclear Physics, Institute of Atomic Energy, Beijing 102413, China.

(Dated: April 8, 2019)

A laboratory has been set up at the Kuo-Sheng Nuclear Power Station at a distance of 28 m from the 2.9 GW reactor core to study low energy neutrino physics. A detector threshold of 5 keV and a background level of $1 \text{ kg}^{-1} \text{ keV}^{-1} \text{ day}^{-1}$ at 12-60 keV were achieved with a high purity germanium detector of mass 1.06 kg surrounded by anti-Compton detectors with NaI(Tl) and CsI(Tl) crystal scintillators. Using 4712 and 1250 hours of Reactor ON and OFF data, respectively, limits of the neutrino magnetic moment of $\mu_{\bar{\nu}_e} < 1.3(1.0) \times 10^{-10} \mu_B$ at 90(68)% confidence level were derived. Indirect bounds of the $\bar{\nu}_e$ radiative lifetime of $m_\nu^3 \tau_\nu > 2.8(4.8) \times 10^{18} \text{ eV}^3 \text{ s}$ can be inferred.

PACS numbers: 14.60.Lm, 13.15.+g, 13.40.Em

The strong evidence of neutrino oscillations from the solar and atmospheric neutrino measurements implies finite neutrino masses and mixings [1, 2]. Their physical origin and experimental consequences are not fully understood. Experimental studies on the neutrino properties and interactions can shed light to these fundamental questions and/or constrain theoretical models. The coupling of neutrinos with the photons are consequences of non-zero neutrino masses. Two of the manifestations of the finite electromagnetic form factors [3] are neutrino magnetic moments and radiative decays. In this paper, we report new limits on these parameters from data of a reactor neutrino experiment taken at a lower energy range than previous measurements.

The searches of neutrino magnetic moments are performed in experiments on neutrino-electron scatterings [4]: $\nu_{l_1} + e^- \rightarrow \nu_{l_2} + e^-$. Both *diagonal* and *transition* moments are allowed, corresponding to the cases where $l_1 = l_2$ and $l_1 \neq l_2$, respectively. The experimental observable is the kinetic energy of the recoil electrons (T). The differential cross section for the magnetic scattering (MS) channel is given by [3]:

$$\left(\frac{d\sigma}{dT}\right)_{\text{MS}} = \frac{\pi \alpha_{\text{em}}^2 \mu_l^2}{m_e^2} \left[\frac{1 - T/E_\nu}{T} \right] \quad (1)$$

where E_ν is the neutrino energy. The neutrino magnetic moment (μ_l), often expressed in units of the Bohr magneton (μ_B), has an $1/T$ dependence and dominates at low electron recoil energy over the Standard Model

(SM) process. The quantity μ_l is an effective parameter which, in the case of $\bar{\nu}_e$, can be expressed as [5]: $\mu_{\bar{\nu}_e}^2 = \sum_j |\sum_k U_{ek} \mu_{jk}|^2$ where U is the mixing matrix and μ_{jk} are the fundamental constants that characterize the couplings between the mass eigenstates ν_j and ν_k with the electromagnetic field. In this paper, we write $\mu_{\bar{\nu}_e} = \kappa_e \times 10^{-10} \mu_B$ for simplicity. The neutrino-photon couplings probed by ν -e scatterings are the same as that giving rise to the neutrino radiative decays [6]: $\nu_j \rightarrow \nu_k + \gamma$ between ν_j and ν_k . The decay rate Γ_{jk} is related to μ_{jk} by: $\Gamma_{jk} = [\mu_{jk}^2 (m_j^2 - m_k^2)^3] / [4\pi m_j^3]$, where m_i is the mass of ν_i .

Reactor neutrinos provide a sensitive probe for “laboratory” searches of $\mu_{\bar{\nu}_e}$, taking advantages of the high $\bar{\nu}_e$ flux, low E_ν and the better experimental control via the reactor ON/OFF comparison. A finite $\mu_{\bar{\nu}_e}$ would manifest itself as excess events in the ON over OFF periods, where the energy spectra have an $1/T$ profile. Neutrino-electron scatterings were first observed in the pioneering experiment [7] at Savannah River. A revised analysis of the data by Ref [3] with improved input parameters gave a positive signature consistent with the interpretation of a finite $\mu_{\bar{\nu}_e}$ at $\kappa_e=2-4$. Other results came from the Kurtchatov [8] and Rovno [9] experiments which quoted limits of $\kappa_e < 2.4$ and < 1.9 at 90% confidence level (CL), respectively. However, many experimental details, in particular the effects due to the uncertainties in the SM “background”, were not discussed. An on-going experiment MUNU [10] is performed at the Bugey reactor

using a time projection chamber with CF_4 gas. A preliminary result of $\kappa_e < 1.3$ (90% CL) was derived, while excess of events below 1 MeV during reactor ON was also reported.

Neutrino flavor conversion induced by resonant or non-resonant spin-flip transitions in the Sun via its transition magnetic moments has been considered to explain the solar neutrino measurements [3], and were recently shown [11] to be consistent with the existing data. Alternatively, the measured solar neutrino ν_\odot -e spectral shape has been used to set limit of $\kappa_\odot < 1.5$ at 90% CL for the “effective” ν_\odot magnetic moment [5] which is in general different from that of a pure ν_e state derived in reactor experiments. Astrophysical arguments [1, 3], placed bounds of $\kappa_{\text{astro}} < 10^{-2} - 10^{-3}$, but there are model dependence and implicit assumptions on the neutrino properties involved.

Further laboratory experiments to put the current limits on more solid grounds and to improve on the sensitivities are therefore necessary. The Kuo-Sheng (KS) results described in this article are based on data taken with an ultra-low-background high purity germanium detector (HPGe) during the period June 2001 till April 2002. The HPGe is optimal for magnetic moment searches [12, 13] with its low detection threshold, excellent energy resolution, and robust stability. The strategy is to focus on energy < 100 keV [14] where the SM background are negligible at the $10^{-10} \mu\text{B}$ range considered here. A CsI(Tl) scintillating crystal array of mass 46 kg was operating in parallel, and data were taken by a single readout system.

The KS neutrino laboratory [12] is located at a distance of 28 m from the Core #1 of the Kuo-Sheng Power Station in Taiwan. The nominal thermal power output is 2.9 GW. The laboratory is at the ground floor of the reactor building at a depth of 12 m below sea-level and with about 25 m water equivalence of overburden. The primary cosmic ray hadronic components are eliminated while the muon flux is reduced by a factor of 4. The laboratory is equipped with an outer 50-ton shielding structure, consisting of, from outside in, 2.5 cm thick plastic scintillator panels with photo-multipliers (PMTs) read-out for cosmic-ray veto (CRV), 15 cm of lead, 5 cm of stainless steel support structures, 25 cm of boron-loaded polyethylene and 5 cm of OFHC copper. The innermost space has a dimension of $100 \times 80 \times 75 \text{ cm}^3$ where both the HPGe and CsI(Tl) detectors and their inner shieldings were placed. Ambient γ -background at the reactor site is about 20 times higher than that of a typical laboratory, predominantly from radioactive dust with ^{60}Co and ^{54}Mn . The dust can get settled on exposed surfaces within hours and is difficult to remove. Some earlier prototype detectors were contaminated by such. Attempts to clean the surfaces on site resulted in higher contaminations. Accordingly, the various detector and inner shielding components were wrapped by plastic sheets during transportation, to be removed on site only prior to in-

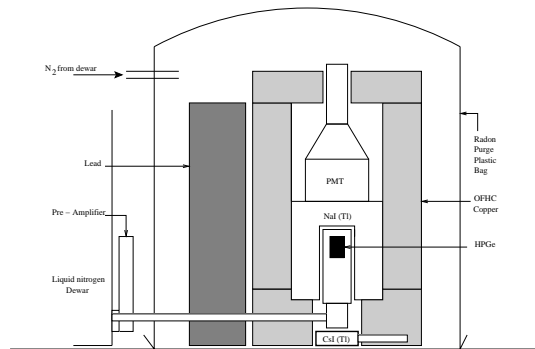


FIG. 1: Schematic layout of the HPGe with its anti-Compton detectors as well as inner shieldings and radon purge system.

stallation. Neutron background is the same as that of a typical surface site, with no observable difference between the ON and OFF period.

The HPGe set-up is schematically shown in Figure 1. It is a coaxial germanium detector with an active target mass of 1.06 kg. The lithium-diffused outer electrode is 0.7 mm thick. The end-cap cryostat, also 0.7 mm thick, is made of OFHC copper. Both of these features provide total suppression to ambient γ -background below 60 keV, such that events below this energy are either due to internal activity or ambient MeV-range γ 's via Compton scattering. The HPGe was surrounded by an anti-Compton (AC) detector system made up of two components: (1) a NaI(Tl) well-detector of thickness 5 cm that fit onto the end-cap cryostat, the inner wall of which is also made of OFHC copper, and (2) a 4 cm thick CsI(Tl) detector at the bottom. Both AC detectors were read out by PMTs with low-activity glass. The assembly was surrounded by 3.7 cm of OFHC copper inner shielding. Another 10 cm of lead provided additional shieldings on the side of the liquid nitrogen dewar and pre-amplifier electronics. The inner shieldings and detectors were covered by a plastic bag connected to the exhaust line of the dewar, serving as a purge for the radioactive radon gas.

The electronics and data acquisition (DAQ) systems of KS laboratory have been described elsewhere [15]. The HPGe pre-amplifier signals were distributed to two spectroscopy amplifiers at the same $4 \mu\text{s}$ shaping time but with different gain factors. A low threshold on the output provided the on-line trigger, ensuring all the events down to the electronics noise edge of 5 keV were recorded. The amplifier and the PMT signals from the AC detectors were recorded by 20 MHz Flash Analog to Digital Converter (FADC) modules for a duration of $10 \mu\text{s}$ and $25 \mu\text{s}$ before and after the trigger, respectively. The discriminator output of the CRV PMTs were also recorded. A random trigger was provided by an external clock at 0.1 Hz for sampling the pedestals and for accurate measurements of the efficiency factors. The DAQ system remained active for 2 ms after a trigger to record possi-

TABLE I: Summary of the event selection procedures as well as their differential suppression and efficiency factors.

Cuts	Suppression	Efficiency
Raw Data	1.0	1.0
Anti-Compton (AC)	0.063	0.994
Cosmic-Ray Veto (CRV)	0.957	0.948
Pulse Shape Analysis	0.860	0.996
Cumulative Net	0.052	0.938

TABLE II: The various contributions to the systematic uncertainties.

Contributions	Uncertainties	$\delta(\kappa_e^2)$
Relative normalization ON/OFF	<0.2%	<0.30
Reactor neutrino spectra	24%	0.23
SM background subtraction	23%	0.03
Efficiencies of MM signal	<0.2%	<0.01
Combined Systematic Error	—	<0.38

ble time-correlated signatures. The typical data taking rate for the HPGe sub-system was about 1 Hz. The DAQ dead time was about 10-20 ms per event and the typical system live time was 96%.

Scatterings of $\bar{\nu}_e$ -e inside the Ge target would manifest as “lone-events” uncorrelated with other detector systems. The selection procedures, suppression factors and efficiencies are summarized in Table I. The AC and CRV cuts suppressed Compton scattering and cosmic-ray induced events. The pulse shape analysis identified background due to electronic noise as well as the delayed “cascade” events. The survival probabilities of the random events along the various stages of the analysis procedures provided accurate measurements of the DAQ dead time and the analysis efficiencies, and allowed corrections to the residual instabilities of the detector hardware. The various residual γ -lines such as that of ^{40}K provided the energy calibration as well as independent consistency checks to the efficiency factors.

The lone-event spectra from for 4712/1250 live time hours of reactor ON/OFF data are displayed in Figure 2a. The relative normalization is known to <0.2%. A detector threshold of 5 keV and a background of $\sim 1 \text{ keV}^{-1}\text{kg}^{-1}\text{day}^{-1}$ above 12 keV were achieved. This is comparable to the typical range in underground Cold Dark Matter experiments. Several lines can be identified: Ga X-rays at 10.37 keV and $^{73}\text{Ge}^*$ at 66.7 keV from internal cosmic-induced activities, and ^{234}Th at 63.3 keV and 92.6 keV due to residual ambient radioactivity from the ^{238}U series in the vicinity of the target. The ON and OFF spectra differ only in one significant feature. There is a difference in the Ga X-ray peaks, which originates from the long-lived isotopes (^{68}Ge and ^{71}Ge with half-lives of 271 and 11.4 days, respectively) activated by cosmic-rays prior to installation. The time evolution of the peak intensity can be fit to two exponentials con-

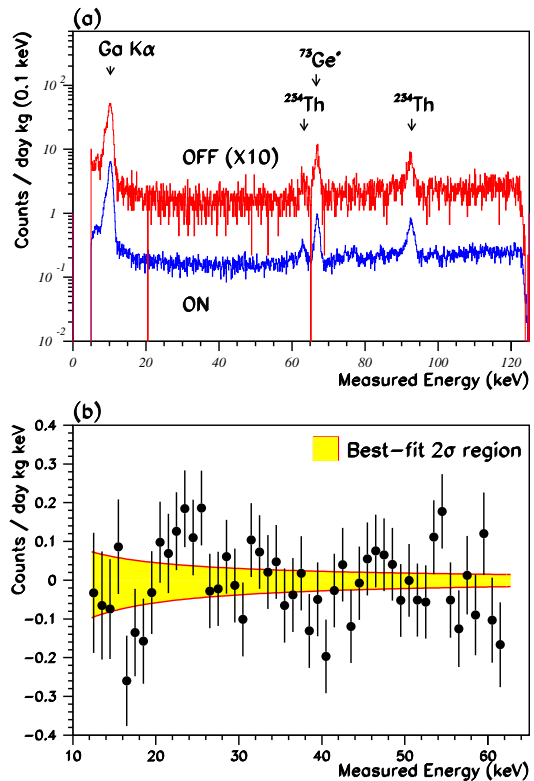


FIG. 2: (a) The energy spectra for lone events, and (b) The residual of the Reactor ON recoil spectrum over ϕ_{OFF} , from 4712/1250 live time hours of Reactor ON/OFF data taking.

tent with the two known half-lives. A threshold of 12 keV was therefore adopted for physics analysis. This is also above the energy range where corrections due to atomic effects have to be considered.

The reactor neutrino spectrum and its time dependence were evaluated from reactor operation data using the standard prescriptions on $\bar{\nu}_e$ from fissions [3] together with a low energy contribution due to neutron capture on ^{238}U [16]. The total flux at the detector is $5.8 \times 10^{12} \text{ cm}^{-2}\text{s}^{-1}$, corresponding to a MS event rate of $5.9 \text{ kg}^{-1}\text{day}^{-1}$ above 12 keV at $\kappa_e = 2$. The uncertainties of the $\bar{\nu}_e$ spectrum at low energy are not well studied [14]. We take the reasonable ranges of 5% and 30% to be the systematic errors above and below 2 MeV, respectively.

The electron recoil spectra from SM and MS interactions at $\mu_{\bar{\nu}_e} = 10^{-10} \mu_B$, denoted by ϕ^{SM} and ϕ_{-10}^{MS} , respectively, were evaluated from $\bar{\nu}_e$ spectrum. The background in the energy range of 12 to 60 keV are due to Compton scatterings of higher energy γ 's. The OFF spectrum was fitted to a 4th-degree polynomial function ϕ_{OFF} , and a χ^2/dof of 80/96 was obtained. The function ϕ_{OFF} and its uncertainties were then used as input to the fit of the ON spectrum to $\phi_{\text{OFF}} + \epsilon(\phi^{\text{SM}} + \kappa_e^2 \phi_{-10}^{\text{MS}})$, where ϵ is the analysis efficiency of Table I. A best-fit value of $\kappa_e^2 = -0.41 \pm 1.28(\text{stat.}) \pm 0.38(\text{sys.})$ at χ^2/dof of 48/49 was obtained. The various systematic errors

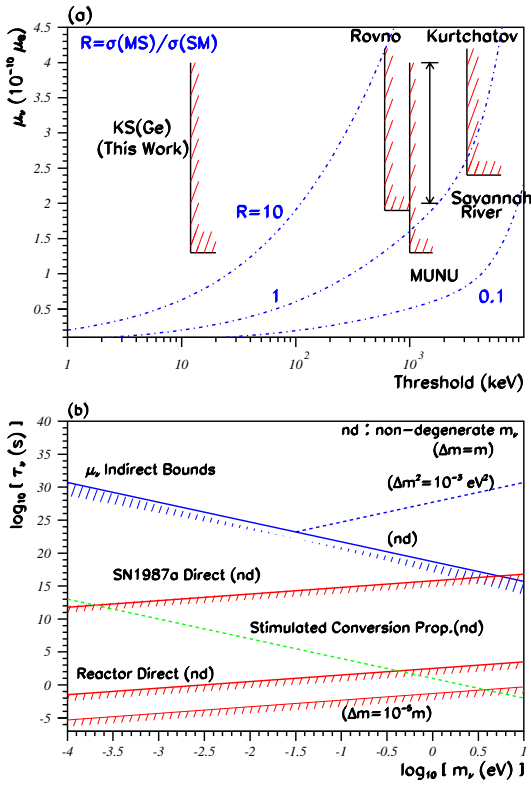


FIG. 3: Summary of the results in (a) the searches of neutrino magnetic moments with reactor neutrinos, and (b) the bounds of neutrino radiative decay lifetime. See text for explanations.

and their contributions to $\delta(\kappa_e^2)$ are summarized in Table II. Following the unified approach [1], the limits on the $\bar{\nu}_e$ magnetic moment of $\mu_{\bar{\nu}_e} < 1.3(1.0) \times 10^{-10} \mu_B$ at 90(68)% CL were derived. The residual plot with the ON spectrum over ϕ_{OFF} and the best-fit 2σ region are depicted in Figure 2b. It has been checked that positive signals with the correct strength and uncertainties can be reconstructed by the procedures from simulated spectra.

Depicted in Figure 3a is the summary of the results in $\mu_{\bar{\nu}_e}$ searches with reactor $\bar{\nu}_e$ versus the achieved threshold. The dotted lines are the $\sigma_{\text{MS}}/\sigma_{\text{SM}}$ ratio at a particular $(T, \mu_{\bar{\nu}_e})$. The KS(Ge) experiment operated at a much lower threshold of 12 keV compared to the other efforts. The large $\sigma_{\text{MS}}/\sigma_{\text{SM}}$ ratio implies that the KS results are robust against the uncertainties in the SM cross-sections. In particular, in the case where the excess of events reported in Refs. [7] and [10] are due to unaccounted sources of neutrinos, the limits remain valid.

Indirect bounds on the neutrino radiative decay lifetimes are inferred and displayed in Figure 3b for the simplified scenario where a single channel dominates the transition, which corresponds to $\tau_\nu m_\nu^3 > 2.8(4.8) \times 10^{18} \text{ eV}^3 \text{ s}$ at 90(68)% CL in the non-degenerate case. Superimposed are the limits from the previous direct searches of excess γ 's from reactor neu-

trinos [17] and from the supernova SN1987a [18], as well as the sensitivity level of proposed simulated conversion experiments at accelerators [19]. It can be seen that ν -e scatterings give much more stringent bounds than the direct approaches.

The KS experiment continues data taking in 2002-03 using HPGe with improved shieldings and 186 kg of CsI(Tl) crystals. Besides improving on the $\mu_{\bar{\nu}_e}$ sensitivities, the goals are to perform a measurement of the $\bar{\nu}_e$ -e cross-section at the MeV range, and to study various standard and anomalous neutrino interactions. A prototype HPGe detector with sub-keV threshold is being studied.

The authors are grateful to their technical staff for invaluable contributions, and to the CYGNUS Collaboration for the veto scintillator loan. This work was supported by contracts 90-2112-M-001-037 and 91-2112-M-001-036 from the National Science Council, Taiwan, and 19975050 from the National Science Foundation, China. H.B. Li is supported by contracts NSC 90-2112-M002-028 and MOE 89-N-FA01-1-0 under P.W.Y. Hwang.

* Corresponding Author: htwong@phys.sinica.edu.tw

- [1] See the respective sections in *Review of Particle Physics*, Particle Data Group, Phys. Rev. **D 66** (2002), for details and references.
- [2] *Proc. of the XX Int. Conf. on Neutrino Phys. & Astrophys.*, Munich, eds. F. von Feilitzsch et al. (2002).
- [3] P. Vogel and J. Engel, Phys. Rev. **D 39**, 3378 (1989), and references therein.
- [4] B. Kayser et al., Phys. Rev. **D 20**, 87 (1979).
- [5] J.F. Beacom and P. Vogel, Phys. Rev. Lett. **83**, 5222 (1999).
- [6] G.G. Raffelt, Phys. Rev. **D 39**, 2066 (1989).
- [7] F. Reines, H.S. Gurr and H.W. Sobel, Phys. Rev. Lett. **37**, 315 (1976).
- [8] G.S. Vidyakin et al, JETP Lett. **55**, 206 (1992).
- [9] A.I. Derbin et al., JETP Lett. **57**, 769 (1993).
- [10] C. Amsler et al., Nucl. Instrum. Methods **A 396**, 115 (1997); J.-L. Vuilleumier, in Ref. [2].
- [11] J. Valle, in Ref. [2], and references therein.
- [12] H.T. Wong and J. Li, Mod. Phys. Lett. **A 15**, 2011 (2000); H.B. Li et al., Nucl. Instrum. Methods **A 459**, 93 (2001).
- [13] A.G. Beda, E.V. Demidova, and A.S. Starostin, Nucl. Phys. **A 663**, 819 (2000).
- [14] H.B. Li and H.T. Wong, J. Phys. **G 28**, 1453 (2002).
- [15] W.P. Lai et al., Nucl. Instrum. Methods **A 465**, 550 (2001).
- [16] V.I. Kopeikin, L.A. Mikaelyan, and V.V. Sinev, Phys. Atomic Nuclei **60**, 172 (1997).
- [17] L. Oberauer, F. von Feilitzsch and R.L. Mössbauer, Phys. Lett. **B 198**, 113 (1987); J. Bouchez et al., Phys. Lett. **B 207**, 217 (1988).
- [18] E.L. Chupp, W.T. Vestrand, and C. Reppin, Phys. Rev. Lett. **62**, 505 (1989).
- [19] M.C. Gonzalez-Garcia, F. Vannucci and J. Castromonte,

Phys. Lett. **B 373**, 153 (1996).